

MD-Alarm: A Novel Manpower Detection Method for Ship Bridge Watchkeeping using WiFi Signals

Mengda Chen, Jie Ma, Xuming Zeng*, Kezhong Liu, Mozi Chen, Kai Zheng, Kehao Wang

Abstract—Sufficient manpower on ship bridges plays an important role in ship navigation and watchkeeping safety. Effectively counting the number of watchkeeping officers and evaluating compliance with manning rules can prevent many ship accidents caused by fatigue and poor lookouts. Current solutions mostly rely on surveillance cameras and watchmen to determine whether to report to the shipmaster, a system that requires extra human effort and raises concerns regarding officers' privacy. In this paper, we utilize WiFi infrastructure in a ship bridge and propose a WiFi-signal-based watchkeeping officer counting method based on fine-grained channel state information (CSI) instead of using cameras. To achieve this goal, we first adopt the Pearson correlation coefficient to evaluate the sensitivity of CSI and extract the CSI subcarriers that are most sensitive to human activities, rather than environmental changes. Then, an expansion matrix algorithm is used to estimate the number of people in the line-of-sight WiFi link using the extracted CSI subcarriers, and a multi-link fusing scheme is proposed to determine the total number of officers in the bridge by using multiple WiFi devices. Finally, after obtaining the number of current watchkeeping officers, combined with the current spatio-temporal properties of the ship, the system determines the number of safe navigation personnel. If the number of people detected does not meet the requirements, the system will issue an alarm. We have conducted extensive experiments in a real-world passenger ship. The experimental results show that after introducing the sensitive subcarrier extraction module, the accuracy of counting the number of officers increased by at least 17%. When the total number was less than 4 or equal to 1, the system achieved an average accuracy of 88% and 94%, respectively.

Index Terms—Ship Bridge Watchkeeping, Crowd Counting, Channel State Information (CSI), Wireless Sensing.

I. INTRODUCTION

Watchkeeping manpower on ship bridges determines the safety of ship navigation [1] [2]. A considerable number of ship collision accidents are caused by insufficient manpower on duty or failure of the pilot on duty to perform the appropriate work [3]. Methods to accurately determine the number of people and detect personnel activity in ship cabs have gained increasing attention, and manpower detection systems are essential in many scenarios. Typical applications

Mengda Chen is with the School of Navigation, Wuhan University of Technology, Wuhan 430063, China (e-mail: chen.mengda@whut.edu.cn).

Kezhong Liu and Jie Ma are with the School of Navigation and Hubei Key Laboratory of Inland Shipping Technology, Wuhan University of Technology, Wuhan 430063, China (e-mail: kzliu@whut.edu.cn; majie@whut.edu.cn).

Mozi Chen, Xuming Zeng and Kai Zheng are with the School of Navigation, Wuhan University of Technology, Wuhan 430063, China (e-mail: chenmz@whut.edu.cn; zengxuming@whut.edu.cn; kzhseng@whut.edu.cn).

Kehao Wang is with the School of Information Engineering, Wuhan University of Technology, Wuhan 430063, China (e-mail: kehao.wang@whut.edu.cn).

*Corresponding author: Xuming Zeng(e-mail: zengxuming@whut.edu.cn).

include detection of people in public places [4], security alarms [5], monitoring of elderly people and children [6] [7], etc. In such applications, it is unrealistic for users to carry specific devices for detection, especially in indoor ship environments. However, detecting the presence of individuals in the target area is critical to the safety of ship navigation. Owing to the unique structural environment of a ship, it is intrinsically challenging to manage people on board. Because of the safety requirements of the cockpit at night, we cannot use video surveillance [8]. However, advances in WiFi techniques have enabled wireless signals to reflect and capture the characteristics of the human body [9]. The primary foundation of this approach is that a person's movement can modulate wireless signals and result in temporal changes that are observable from the received signals [10]. Pioneering efforts have explored the possibility of extracting motion information from wireless signals to localize [11] or track body movements or even respiratory rates.

Earlier pioneering work has employed various techniques and measurements, among which the received signal strength (RSS) is one of the most popular. Using this approach, it is possible to extract relevant features from wireless devices [12]. However, RSS-based detection schemes are limited by their accuracy, and coarse-grained schemes cannot meet the requirements of certain circumstances. In particular, the steel structure in a ship environment will have a significant impact on the signal [13]. As a result, false detections can occur frequently because the RSS changes. Fortunately, CSI has been excavated recently. CSI extracted from the WiFi physical layer can provide fine-grained information on multiple channels, which significantly improves accuracy. CSI contains amplitude and phase information, whereas the RSSI has only an average signal strength value for each packet [14].

However, raw CSI measurements cannot be directly applied to crowd counting because of the strong multipath propagation, hardware noise, and limitations of wearable devices [15] [16]. Consequently, previous approaches were difficult to use in indoor ship environments [17] [18] [19]. Although there has been a lot of recent work on the use of WiFi signals for crowd counting, most of them have not considered the performance of the system in a dynamic steel structure indoor environment similar to the interior of a ship [20] [21] [22]. Past research shows that factors such as the spatial structure of the ship and the movement of the hull cause interference with CSI [23]. This poses a challenge to crowd counting in indoor ship environments. Considering diversity in human behavior, especially in terms of walking speed, the false alarm rate might be high [24]. Benefiting from the full advantages of CSI, we

found independent subcarriers that have different sensitivities to the environment, thus filtering CSI information that is more sensitive to personnel activities in the complex environment of a ship's interior.

Note that computer vision was the first method to be applied to crowd counting [25], and by extracting features from the fixed image mode, this technique can identify images accurately. However, computer vision is not applicable in many scenarios, and light intensity changes or video blind spots will have a significant influence. By deploying a large number of infrared sensor nodes inside the area, we could collect data for behavior recognition. Although this approach has good adaptability to the environment, the deployment cost is high and maintenance is difficult, and it is also limited by the line-of-sight propagation path. On the other hand, ultra-wideband technology [26] has emerged in the field of wireless networks. Although it is insensitive to channel fading and has low signal power spectral density, it requires special equipment, and is expensive and unsuitable for lightweight crowd counting.

In this paper, we propose a novel solution for crowd counting in a ship environment, which can accurately detect the number of active people at a low cost in an indoor ship environment. In contrast to previous works, we propose the concept of sensitive subcarriers (SSCs) and add a selecting process for SSCs to the system. While reducing redundant calculations to improve the detection efficiency, extracting the CSI subcarrier sequence that is more sensitive to the ship's indoor personnel activities will make the number of people detected more precise. By processing the selected wireless signals with the expansion matrix algorithm [27], our system can estimate the number of active persons; at the same time, it also imposes implicit requirements for the on-duty personnel to have a certain degree of effective activity. The main contributions of this paper include:

- 1) We design a novel system to detect watchkeeping manpower in ships' bridges. By filtering and utilizing CSI signal features that are more sensitive to human activities, complex environmental information that is not related to human activities can be filtered to the maximum. Even in a dynamic multipath environment can have a good detection effect.
- 2) We analyze actual ship data to prove the sensitivity difference of CSI subcarrier sequences of different frequencies for personnel activities between ship navigation, we propose the concept of sensitive subcarriers(SSCs) and propose an evaluation method for selecting sensitive subcarriers for different targets.
- 3) We perform an experimental evaluation and algorithm verification for the designed system, extensive experiments demonstrate the system has good results even when used on mobile ships.

II. MOTIVATION AND OBSERVATION

According to the post-investigation and analysis of ship accidents, it has been confirmed that during the process of vessel operation, low manning (usually considered to be no more than two people) will cause watchkeeping officers to

become fatigued and render the captain unable to perform their duties, which in turn often leads to accidents [1]. As shown in Fig. 1, 45% of accidents are caused by non-standard driving behaviors. Among them, reasons related to the lack of manpower in terms of on-duty watchkeepers account for a considerable proportion. For example, having poor or no lookouts and one-man bridge operations accounted for 23% and 7% of accident causes, respectively. Therefore, we believe that effective constraints on the number of driving configurations for ship driving can significantly reduce the probability of various ship collision accidents.

At present, the supervision of ship drivers is mainly based on onboard indoor camera equipment and human supervision of the monitoring center. Although this method is simple and straightforward, it also has some shortcomings that cannot be ignored. First, to clearly identify the channel indication facilities during night navigation, the lighting equipment in the cab must be turned off to eliminate the influence of light, which makes the indoor camera equipment unable to reflect complete and reliable image information, and the personal privacy of the driver is greatly compromised. In recent years, this system has also been widely resisted by ships' crews. Second, the supervision model based on machine vision is usually accompanied by a certain cost for independent equipment and manpower supervision [28]. Therefore, there is a need for a lightweight crowd counting system that does not need to rely on image and video information, has high privacy, and is inexpensive.

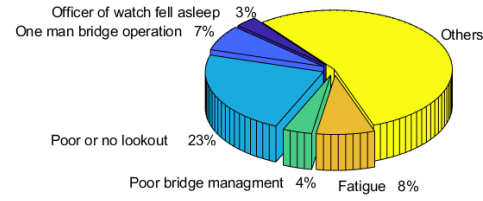


Fig. 1. Attributed causes of collisions Feature.

A. Channel State Information for Human Perception

Channel state information (CSI), as physical layer information, contains significant channel information that is not visible to the media access control layer, and describes the state of each channel in the signal propagation process in a more granular manner [29]. Compared with RSSI, which contains a large number of multipath effects superimposed on a comprehensive value, CSI obtains a multi-group subcarrier matrix composed of a pair of transmitting and receiving antennas. The CSI obtained by the different subcarriers exhibit different degrees of fading [30]. CSI extends a single RSSI value to the frequency domain and can also reflect the phase information of the signal. In different environments, CSI shows different amplitude and phase characteristics, providing more fine-grained information for the perception of the environment. Compared with RSSI, CSI also has better environmental stability; therefore, through

some signal processing methods, we can extract richer and more robust signal features from CSI, and more accurately perceive the environment. A compatible IEEE 802.11 wireless network card can obtain a set of CSI from each received data packet. The wireless network card uses the CSI that characterizes the frequency response of the wireless channel to continuously monitor changes in the wireless channel. The frequency response formula is as follows:

$$Y(f, t) = H(f, t) \times X(f, t) \quad (1)$$

where $Y(f, t)$ and $X(f, t)$ are the frequency-domain representations of the signal at the receiving and transmitting ends, respectively. $H(f, t)$ is the channel frequency response (CFR) at time t , which is a complex value. Each group of transmitting and receiving antennas forms a signal link, and a data packet transmitted by each link contains CFR sampling information of $N = 30$ subcarriers.

$$H(f_k) = [H(f_1), H(f_2), \dots, H(f_N)] \quad (2)$$

The channel frequency response of a single subcarrier can be expressed as:

$$H(f_k) = \|H(f_k)\| e^{j\angle H(f_k)} \quad (3)$$

In this formula, $H(f_k)$ is the CSI information of the k -th subcarrier with the center frequency of f_k , $\|H(f_k)\|$ is the amplitude information of the subcarrier, and $\angle H(f_k)$ is the phase information of the subcarrier; however, owing to the random noise between the transmitting antenna and the receiving antenna and the desynchronization of time, the acquired original phase information appears very random and cannot be directly applied. The measured phase of the i -th subcarrier can be expressed as

$$\hat{\phi}_i = \phi_i - 2\pi \frac{k_i}{N} \delta + \beta + Z \quad (4)$$

where ϕ is the true phase, δ is the time offset, β is the phase offset, Z is the noise interference, k_i is the subcarrier label, and N is the length of the fast Fourier transform (in IEEE 802.11, k_i is -288 and N is 64). To make full use of the phase information, the original phase needs to be processed to eliminate these significant offset components. If the subcarrier frequency is symmetric, the original phase can be linearly transformed by formula (5) to obtain a linear combination of the true phase, and the random phase shift is eliminated (ignoring the weak noise Z).

$$\tilde{\phi}_i = \phi_i - \frac{\phi_n - \phi_1}{k_n - k_1} k_i - \frac{1}{n} \sum_{j=1}^n \phi_j \quad (5)$$

We visualized the CSI signals under different personnel activities in the wheelhouse of the ship. We used one WiFi transmitter and three receivers, two Lenovo PCs equipped with off-the-shelf Intel 5300 WiFi cards as transmitters and receivers on the Golden Six cruise ship, which sailed between Chongqing and Yichang (China). In our experiment, the sampling rate of CSI was set to 100 Hz. We set up a single-link

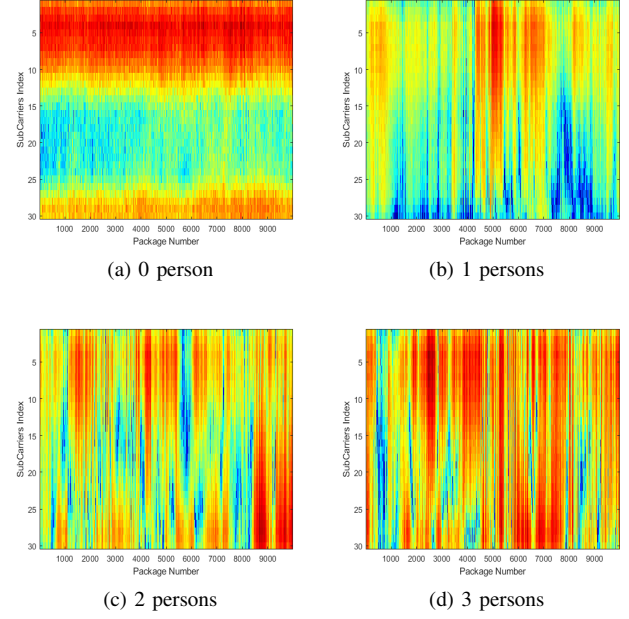


Fig. 2. CSI measurements value of 30 SCs with different numbers of moving people in the indoor environment of the sailing ship.

WiFi environment in the ship's bridge, and arranged 0-3 experimenters to perform typical watchkeepers' activities within the signal range, as shown below, each record contains the content of 1000 CSI data packets. Observing the distribution of CSI amplitude values in Fig. 2, it can be seen that with an increase in the number of moving people, the distribution range of CSI amplitude values becomes wider and the fluctuations become more severe. When the number of people increases from one to three, the difference is particularly obvious. This proves that it is feasible to estimate the number of people in a small crowd using CSI data.

B. CSI Characteristics in Ship Environments

In contrast to ordinary indoor environments, many wireless sensing technologies cannot work normally in a ship owing to the special internal structure and navigation factors of the ship. The steel structure of a ship increases the scattering and absorption of the signal during the propagation process [13]. In addition, the energy loss and hull vibration caused by the ship's navigation will also cause instability in the signal propagation, and the signal instability of a ship environment is much higher than that of an ordinary indoor environment. In Fig. 3(c)(d), we compared the CSI signal time-domain feature, CSI spectrum, amplitude variances of mobile ships(including Sailing state and Pre-sailing state) and ordinary laboratories. There is no human activity in the scene when the signal is collected, as shown in Fig. 3(a)(b).

It is not difficult to see that the CSI signal characteristics under different indoor environments are significantly different. The difference in CSI signal amplitude, variance, and CSI spectrum characteristics will become more obvious with the gradual change of the environment. When the ship starts to speed up, the difference in the ship's indoor signal

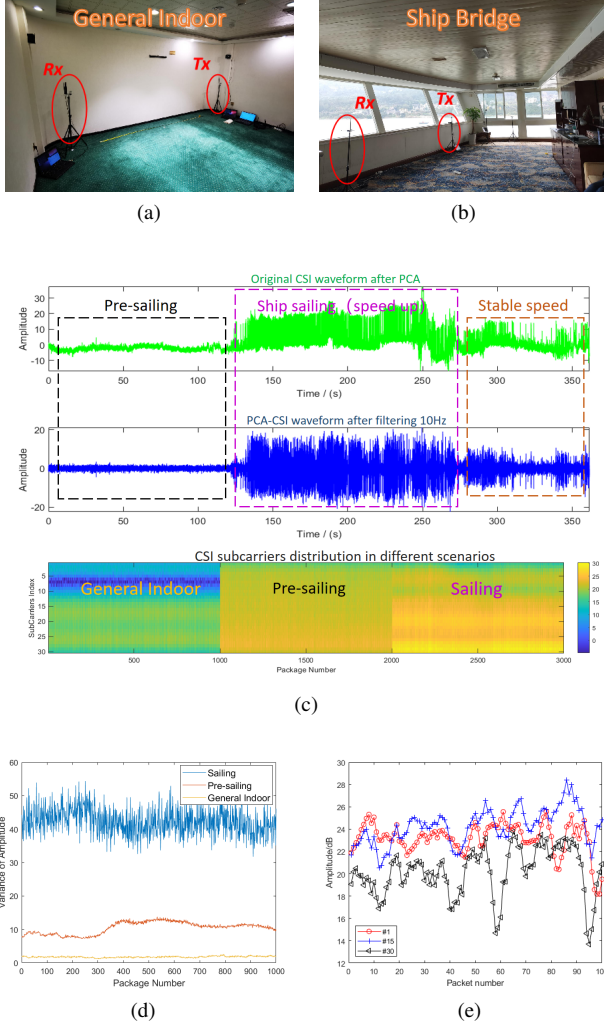


Fig. 3. (a) Layout of an unmanned CSI data collection device in a general indoor scenario. (b) Layout of an unmanned CSI data collection device in a ship bridge scenario. (c) CSI signal characteristics under different motion states and scenarios of ships. (d) Variation of amplitude between the laboratory and shipboard indoor environment. (e) Amplitude comparison for partial subcarriers on ship bridge.

characteristics reaches the maximum. When the ship's speed stabilizes or is in the pre-sailing stage, this signal characteristic difference will be weakened, but it is still significantly higher than the non-dynamic normal indoor environment. How to distinguish and filter environmental information unrelated to human activities will be our challenge.

In an ideal environment, the attenuation of the signal in the reflection and refraction is related to the signal frequency, which is as follows:

$$d = \frac{1}{4\pi} \left[\left(\frac{c}{f_0 \times |\text{CSI}_{\text{eff}}|} \right)^2 \sigma \right]^{\frac{1}{n}} \quad (6)$$

where c is the speed of light, σ is the environmental variable, and n is the path fading index. The values of σ and n are different in different indoor environments and need to be obtained through empirical measurements. The environmental variable σ represents the gain from the baseband to the RF band at the transmitter, the gain from the RF band to the baseband at the receiver, and the antenna gain. Compared with low-frequency signals, high-frequency signals experience more severe fading. If the separation between the two subcarriers is greater than the coherence bandwidth, they will fade independently. The channel bandwidth of 802.11n is larger than the coherent bandwidth in an indoor environment. Therefore, different subcarriers exhibit frequency-selective fading. Fig. 3(e) depicts the impact of individual behaviors on independent subcarriers. Even if the propagation environments of the three groups of subcarriers are identical, they still show significant differences. Among them, the 30th subcarrier is compared with the 1st subcarrier, and the 15th subcarrier is more sensitive.

The analysis of the phase information can start from the channel impulse response of the CSI. We use the Inverse Fourier Transform to convert the channel frequency response containing the phase-frequency characteristics into the channel impulse response. Comparing the CSI channel impulse response distributions under different numbers of people, we find that when the number of people is small, the time to reach the peak of the energy value is shorter, and the energy value distribution is more uniform. When the number of people is large, the peak energy value is higher, the arrival time will be later, the energy distribution will become uneven, and there will be a sudden decrease in energy. Through the analysis of the experimental samples, we found that the CSI channel impulse response with a small number of people has a shorter average excess delay than when the number of people is large. Therefore, the average excessive delay can effectively evaluate the number of active people in the signal propagation environment.

The above analysis found that: (1) a ship environment causes more noise interference to the signal compared with an ordinary indoor environment; (2) the sensitivity of different subcarriers (SCs) of CSI to different targets is different. Therefore, improving the accuracy of human detection in the ship environment by using the sensitivity difference of SCs while weakening the environmental noise interference is the key issue to be addressed in this study.

III. SYSTEM OVERVIEW

The system obtains the CSI measurement value from the existing WiFi physical layer information and estimates the number of people by quantifying the overall activity of the crowd. The system uses less CSI data to reflect the degree of personnel activity to the greatest extent, so it can also shorten the time required for identification. The system is composed of the three modules shown in Figure 4.

Pre-processing Module: After the detection scenario is determined, the system will select sensitive subcarriers over a short period of time, and upload these groups of subcarriers with different numbers for subsequent processing as required. At the same time, the system performs phase sanitization [31] [32], outlier filtering, and interpolation processing [33] on the CSI data.

Crowd Counting Module: Based on the feature extraction results of the personnel activity state, the system combines the personnel motion model with the expansion matrix method

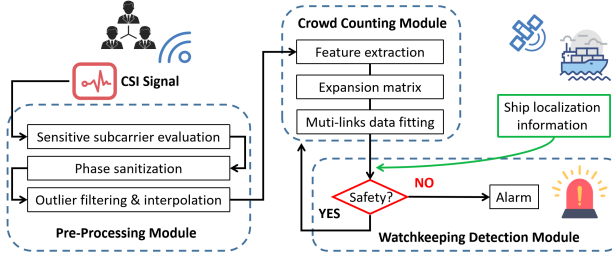


Fig. 4. System overview of MD-Alarm.

to quantitatively describe the overall personnel motion state, thereby completing the estimation of the group number. In addition, to correct the repeated detection of the same target in a multi-link scenario, the system performs data fitting processing on the results of all links.

Watchkeeping Detection Module: Finally, the system uses ship localization data as a reference for the safety of the number of people on duty, and evaluates whether the current number of people on duty meets the safety level requirements of the current channel section. If the number of people on duty does not meet the safety requirements, the system will issue an alarm. Finally, the system returns to the previous stage of the process and cyclically processes the data.

IV. PRE-PROCESSING CSI MEASUREMENT

A. CSI Subcarrier Correlation

The sensitivity of independent SCs to the environment varies. If all SCs are used for human activity detection, some SCs that are not sensitive enough to the environment may mask the influence of the movement of people in the environment on the signal. Therefore, it needs to be filtered out. Personnel activity detection is performed on the SCs with higher environmental sensitivity. This paper proposes an SC sensitivity evaluation model, through which the distribution differences of different subcarriers are quantified, and the SCs that are more sensitive to human activity can be selected in advance to improve the accuracy of manpower detection.

The Pearson correlation coefficient (PCC) is a coefficient that reflects the degree of linear correlation between two quantities. This value is often represented by the lowercase letter r . The r -value ranges from -1 to 1. The closer the absolute value is to 1, the stronger the correlation (negative or positive).

We generally use Euclidean distance (the distance between vectors) to measure the similarity of vectors, but Euclidean distance cannot take into account the difference in values between different variables. Generally, we can prioritize using the standardized Euclidean distance or other distance measures in low dimensions. The Pearson correlation coefficient is more suitable in high dimensions. Therefore, we adopt the PCC method to construct the sensitive subcarrier model.

B. Subcarrier Sensitivity Evaluation Model

To characterize the differences between the sensitivities of different subcarriers, we choose to separately analyze the

correlation between active personnel and sailing ships relative to CSI signals. We construct a motion feature model for a certain period of time using environmental sensor data and collect CSI data under the same time window. The correlations of the subcarriers of each frequency with the sensor motion feature model are compared. Thus, more sensitive subcarriers are obtained as inputs for human detection. The specific process is as follows.

First, we can define $P = [B, V, A_x, A_y, A_z, C, P, M, S]$ as the environmental motion matrix and perform sensor data collection. Here, B is the light intensity, V is the linear acceleration, A_x is the X-axis acceleration, A_y is the Y-axis acceleration, A_z is the Z-axis acceleration, C is the geographic direction angle, P is the atmospheric pressure, M is the magnetic field strength, and S is the sound strength. In addition, we collect the CSI data in this environment as a reference, including 30 sets of amplitude and phase data including 30 subcarriers, and obtain the probability density distribution matrix $Q = [Q_1, Q_2 \dots Q_{30}]$ of 30 subcarriers.

Based on the time-varying nature of the sensitive subcarriers obtained in the previous section, in order to prevent the subcarriers from changing in the selected time period, 30 shorter data packets are selected as the sliding time window, and the CSI dataset for each sliding time window, containing 30 groups of 30 subcarriers, is represented by a 30×30 matrix. Furthermore, 30 groups of sensor data packets in the same time window are selected to construct the corresponding probability density distribution matrix $P = [P_1, P_2 \dots P_{30}]^T$.

$$Q = \begin{bmatrix} CSI_{1,1} & CSI_{1,2} & \dots & CSI_{1,30} \\ CSI_{2,1} & CSI_{2,2} & \dots & CSI_{2,30} \\ \vdots & \vdots & \ddots & \vdots \\ CSI_{30,1} & CSI_{30,2} & \dots & CSI_{30,30} \end{bmatrix} \Rightarrow [Q_1 Q_2 \dots Q_{30}] \quad (7)$$

$$P = \begin{bmatrix} B_1 & V_1 & \dots & S_1 \\ B_2 & V_2 & \dots & S_2 \\ \vdots & \vdots & \ddots & \vdots \\ B_{30} & V_{30} & \dots & S_{30} \end{bmatrix} \Rightarrow [P_1 P_2 \dots P_{30}] \quad (8)$$

By comparing the correlation between the CSI data distribution collected in the test phase and the environmental sensor data distribution, it is possible to determine which subcarriers are more sensitive to environmental factors. The comparison process uses the PCC to measure the difference. The specific process is as follows:

$$\rho(k) = \frac{\text{cov}(P_i(k), Q_i)}{\sigma_{P_i(k)} \sigma_{Q_i}} = \frac{E((P_i(k) - \mu_{P_i(k)})(Q_i - \mu_{Q_i}))}{\sigma_{P_i(k)} \sigma_{Q_i}} \quad (9)$$

The subcarrier sequence number K ranges from 1 to 30, and the sensor data serial number i ranges from 1 to 9. Through this method, the correlation evaluation results of the personnel and ships on each subcarrier are obtained. After removing the data with low correlation, principal component analysis (PCA) is used to process the data and reduce the dimensionality,

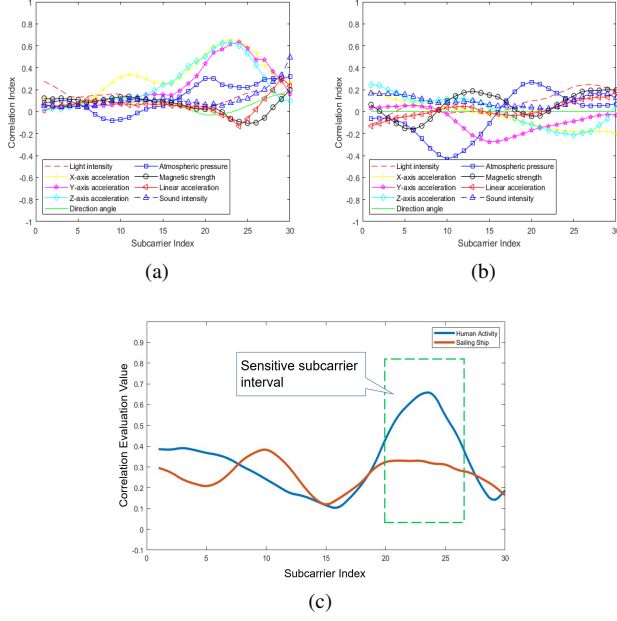


Fig. 5. (a) Correlation analysis of CSI data and various sensor data on active personnel. (b) Correlation analysis of CSI data and various sensor data on sailing ships. (c) Sensitivity analysis of activity personnel and sailing ship for each CSI subcarrier.

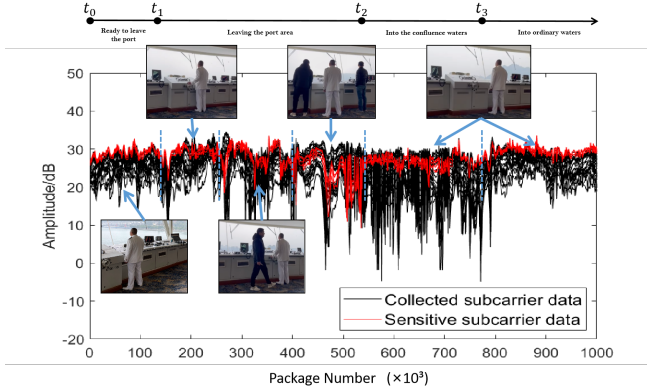


Fig. 6. Schematic diagram of sensitive subcarriers selected.

which can more intuitively select out the factors affecting the subcarrier sequence with greater impact.

V. SYSTEM DESIGN

A. Feature Extraction and Classification

The advantage of principal component analysis is that it can eliminate the singularity of the data and extract the most important features of the original data. This study attempts to find such a set of basis vectors that can represent the original CSI data and retain the environmental information in the original data. By combining the amplitude and phase characteristics of CSI, we can perform manpower detection. The feature extraction process used in this study is as follows:

(1) First, extract K (usually selected as 30) sets of continuous CSI data from a specific time window, and obtain the amplitude and phase matrices H and ϕ , both of which are

$K \times 30$ matrices containing 30 subcarriers and K data packets. Because the attenuation of the signal is related primarily to the frequency of the subcarrier, the amplitude value of the subcarrier of the unpassable frequency is first standardized.

$$H'(f_k) = \frac{f_k}{f_c} \cdot H(f_k) \quad (10)$$

where f_c is the carrier center frequency, f_k is the k-th subcarrier frequency, $H(f_k)$ is the initial frequency, and $H'(f_k)$ is the standardized frequency representation.

(2) Normalize the amplitude and phase matrices, find the largest element H_{max} and the smallest element H_{min} in the copy matrix, then replace each element in the matrix with

$$\bar{H} = \frac{H - H_{min}}{H_{max} - H_{min}} \quad (11)$$

The phase matrix uses the same normalization method.

(3) $\|\bar{H}\|$ and $\bar{\phi}$ are the normalized amplitude and phase matrices, respectively, and their respective covariance matrices are calculated as follows:

$$\begin{cases} \sum(\|\bar{H}\|) = [cov(\bar{H}_i, \bar{H}_j)]_{K \times K} \\ \sum(\bar{\phi}) = [cov(\bar{\phi}_i, \bar{\phi}_j)]_{K \times K} \end{cases} \quad (12)$$

These two covariance matrices reflect the correlation of the data between the K dimensions. The smaller the covariance, the lower the degree of personnel activity.

(4) After the two sets of covariance matrices are obtained, in order to further obtain more easily categorized features, singular value decomposition is used to obtain the eigenvalues and eigenvectors of the two covariance matrices.

$$svd(\sum(\|\bar{H}\|)) = U \begin{bmatrix} \lambda_1 & & & \\ & \lambda_2 & & \\ & & \ddots & \\ & & & \lambda_k \end{bmatrix} V^T \quad (13)$$

We obtain the CSI amplitude and phase eigenvalue vectors λ_H and λ_ϕ , respectively. These two sets of eigenvectors contain most of the information of the amplitude and phase matrices, and are K-dimensional eigenvectors. After filtering out the redundant data, the two sets of amplitude and phase eigenvalue vectors are finally obtained, and the maximum values $\alpha = \max(\lambda_H)$ and $\beta = \max(\lambda_\phi)$ are selected as the classification feature inputs.

After obtaining the characteristic value data under the two categories of no people active and people active, the use of a suitable classification algorithm to accurately divide the two categories and establish an effective classification model is also a key technical part of the personnel movement detection algorithm. Different classification algorithms may have different definitions for the same situation. After comprehensively considering multiple methods, in this study, we chose the support vector machine (SVM) as the main classification algorithm. Based on the large amount of feature value data that have been obtained with and without human movement, the support vector machine algorithm can be used directly to construct the classification model.

B. Crowd Counting

The difficulty in implementing the method of estimating the number of personnel based on CSI lies in finding the mapping between the change in the number of personnel and the change in the CSI caused by that change. This mapping is also based on the feature value extracted from the CSI data and must be between the number of personnel [20]. There is a certain monotonic relationship between these factors. After a series of comparative experiments, we found that when people are moving in the area between the transmitting and receiving antennas, the people may block the signal propagation path, resulting in signal reflection and diffraction. Each person can be regarded as a virtual source, these virtual sources form signal reflections and fading, and ultimately increase or decrease the amplitude of the signal.

However, the receiver cannot directly distinguish which path the received signal comes from, because the propagation distance of the signal is too short and the time resolution is too small to distinguish each path, and the signal in the environment is affected not only by the reflection of human bodies. The surrounding walls and obstacles also reflect the signal.

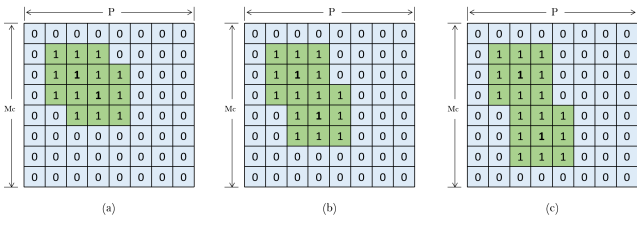


Fig. 7. Matrix expansion diagram.

The algorithm we designed is based on mathematical morphology [27], it is divided into offline phase and test phase. The first phase is to collect CSI data under different numbers of watchkeepers and then extract their frequency domain characteristics-matrix expansion coefficient. signal feature quantities are built to fit regression models to construct a fingerprint database that matches the number of watchkeepers. In the second phase, the CSI data of the unknown number of personnel is collected, and after the frequency domain features are extracted, they are compared and analyzed with the features in the fingerprint library to obtain the Estimated result of the current number of watchkeepers.

To accurately characterize the amplitude value change characteristics of CSI, this study uses the expansion matrix algorithm, which is also based on the influence of changes in the number of personnel on the amplitude value fluctuation of CSI information. When the number of personnel is small, the CSI amplitude value fluctuates less and the distribution of the amplitude value is more concentrated. When defining an amplitude value distribution space, the distribution of amplitude values occupies a relatively small portion in this space. When the number of personnel increases, the CSI amplitude value fluctuates more intensely, the distribution range of the amplitude value is wider, and the distribution range occupies a larger proportion of the amplitude value space.

Step 1: First, define the expansion matrix M_0 based on the amplitude value of the CSI data. The matrix dimension is $M_C \times P$, where P represents the number of CSI data packets received; M_C is the matrix resolution, which is the amplitude value space mentioned above; and the interval is defined by the user. The larger its value, the higher the resolution of the CSI amplitude value, which makes the algorithm more accurate, but an excessively large value of M_C will affect the efficiency of the algorithm. In the initial matrix, all $M_C \times P$ elements are initialized to 0. When the amplitude value of the i -th CSI data packet is obtained, the amplitude value $C[i](i = 1, 2, \dots, n)$ is converted to k using formula 14.

$$k = \left[\frac{c_i - c_{min}}{c_{max} - c_{min}} \times (M_c - 1) \right] + 1 \quad (14)$$

then, change the value of the k -th row element in the i -th column of the matrix from 0 to 1; finally, a total of P such k values are obtained. Only one 0 in each column of the matrix M_0 is changed to 1. Obviously, when the CSI amplitude value changes drastically, the difference in the k values calculated from the amplitude values of two adjacent packets will be larger. At this time, the two adjacent columns in the matrix M_0 are set to 1. The number of rows of elements (k) difference will also be greater.

Step 2: Change the values surrounding the elements that have been changed from 0 to 1. We call this step the expansion of the matrix. Set R as the expansion radius of the matrix, indicating that this value is set to 1 element range. At this time, the matrix M_0 of CSI becomes M . As shown in the Fig. 7, all grids in the figure can be regarded as matrix M_0 . The grid shown as 1 represents the element that was set to 1 in the first step, and it surrounds the grid. The shaded area of is the matrix expansion that causes all elements surrounding the 0 element to be set to 1. At this time, the area of elements set to 1 will overlap. When the number of people in the environment is small, the difference in the CSI amplitude of different packages decreases, and the calculated k value gap also decreases. If the element line difference set to 1 is 1, then a large overlap area is formed after expansion, and the proportion of the requested area decreases accordingly, as shown in the shaded part of Fig. 7(a). As the number of personnel increases, the CSI amplitude value changes more drastically, and the overlapping area of elements set to 1 in matrix M will decrease, resulting in most elements in matrix M_0 being set to 1. Fig. 7(b) and 7(c) show the process in which the fluctuations become more intense. As the overlapping area decreases, the shaded part becomes larger, and the proportion of the total area increases accordingly.

Step 3: Finally, count the number of elements in the matrix M that are equal to 1, and calculate their percentage PER in the population. If more areas overlap in the matrix expansion, the portions of the matrix set to 1 have fewer elements and account for a smaller percentage of the overall population. This percentage is used to map the number of people in the monitoring area. We randomly selected the percentage PER coefficient of a subcarrier, as shown in Figure 9. As the number of people increases, the percentage coefficient increases from 0.36 to approximately 0.53, showing an overall upward trend.

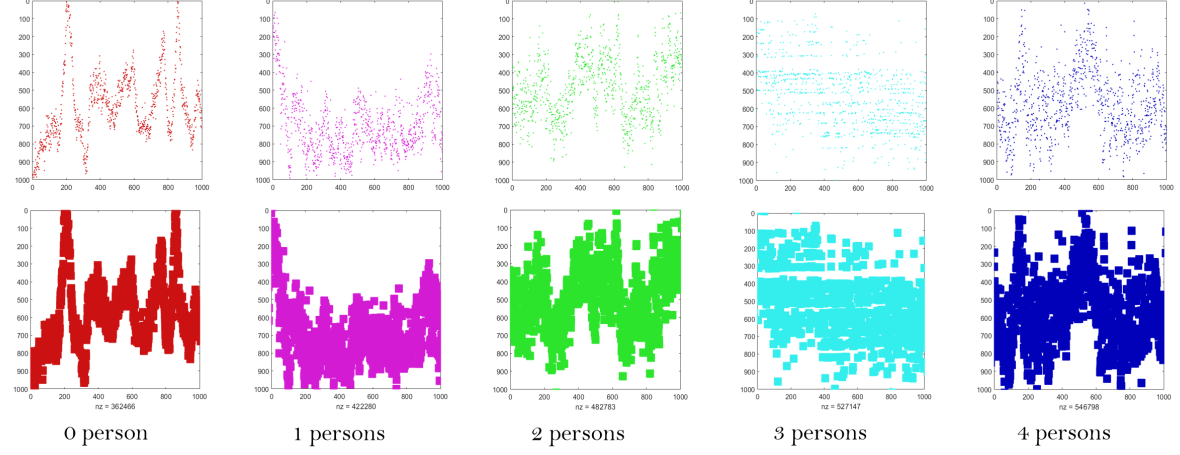


Fig. 8. Matrix expansion process for different numbers of people. As the number of personnel increases, the CSI amplitude value changes more drastically, and the overlapping area of elements set to 1 in matrix M will decrease, resulting in most elements in matrix M_0 being set to 1. As the overlapping area decreases, the shaded part becomes larger, and the proportion of the total area increases accordingly. Eventually caused an increase in the PER value.

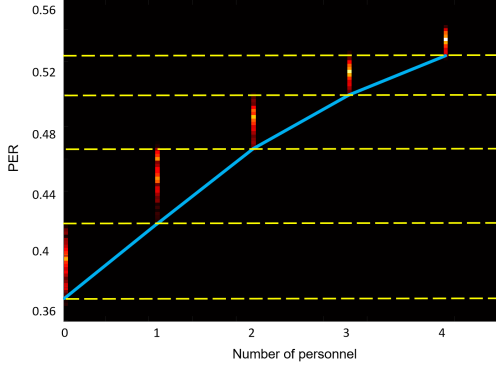


Fig. 9. PER under different numbers of personnel.

However, we know that the percentage coefficient cannot continue to rise. In fact, when the number of personnel reaches a threshold, the impact on the CSI amplitude value will also reach an upper limit, resulting in the percentage PER no longer increasing with the increase in the number of personnel. This is also a limitation of the current technology for detecting the number of people based on wireless perception, but lightweight personnel estimation is nonetheless sufficient for the daily management needs of ships.

C. Multi-link Scenario Design

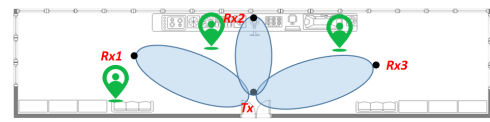
When the active personnel are far away from the WiFi link, the signal fluctuations reflected by the CSI data are affected by the distance of the personnel and cause varying degrees of weakening. When the detection space is large and only a single WiFi link is used for identification, this phenomenon will inevitably lead to inaccurate detection results. For example, when one person is active in the LOS area and one is active in the NLOS area, the target person in the NLOS area will be. The reflected CSI signal has low fluctuation and cannot be detected by the system smoothly. To solve this problem, we recommend using the multi-link deployment method in larger experimental scenarios to expand the detection range



(a) One-link



(b) Two-link



(c) Three-link

Fig. 10. Experimental design under different WiFi link scenarios.

and eliminate long-distance weakening, as shown in Figure 10.

On the other hand, when we use a multi-link scenario design, a given active person will have a certain degree of influence on the CSI data of each link, as shown in Figure 11. If we simply accumulate the PER value of each link as the basis for estimating the number of people, it will eventually lead to repeated calculations of the personnel target. If the maximum/minimum value of the calculation result of each link is used for personnel estimation, the CSI information of all links cannot be reflected, resulting in insufficient personnel estimation.

To preserve the CSI information reflected by all links to the greatest extent and avoid repeated statistics of personnel, based on the linear characteristic analysis of the PER value in the previous chapter, we designed a model to complete the multi-link data correction:

$$PER_n = \omega_1 \sum_{i=1}^n PER_{Rx_i} + \omega_2 PER_{low} \quad (15)$$

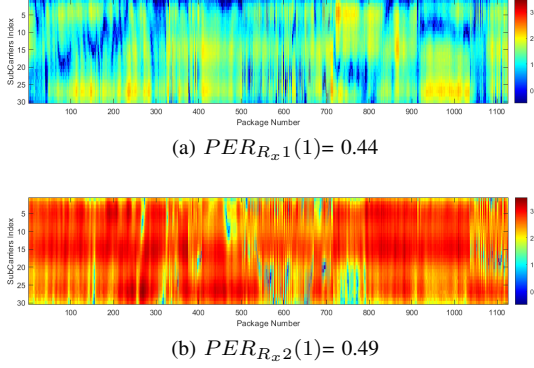


Fig. 11. CSI signal amplitude changes reflected by Rx_1 and Rx_2 when a person is walking in the Rx_2 to Tx link region in a two-link scenario. After calculation, the PER calculated by Rx_1 is approximately 0.44, and the PER calculated by Rx_2 is approximately 0.49, both of which reflect the recognition of personnel activities to a certain extent.

For this formula, the constants ω_1 and ω_2 are obtained through machine learning, and they vary with the layout of multi-link experiment scenarios (affected by factors such as the length of a single link and the angle between each link). PER_{low} is the lower bound value of the PER basis, namely, the minimum PER of a single link in an unmanned environment.

D. Navigation Safety Precaution

In the actual navigation process, the minimum number of safe personnel in the cockpit usually varies according to the area in which the ship is located. For example, in some ocean routes with open waters and long distances between ships, navigation requirements can be met by ensuring that the helmsmen and watchmen are on duty. In some inland waterways with complex navigation environments and high density of ships, it is usually necessary to ensure the presence of helmsmen, watchmen, captains, chief mates, and other personnel to ensure the safe navigation of ships. Therefore, we import ship positioning information for this system to serve as the basis for inspection standards for ship cockpit personnel. By adding this link in the system, the navigation safety inspection process of this system is combined with the information of actual situations, and the more rational judgments can be made.

VI. IMPLEMENTATION

To evaluate the accuracy of the personnel activity detection algorithm includes the effect of sensitive subcarrier filtering and the system's detection of the number of people active in the ship's cockpit. We carried out an experiment on the Golden Six cruise ship, which sailed between Chongqing and Yichang (China). Our system requires a WiFi transmitter and three receivers. We used two Lenovo PCs equipped with off-the-shelf Intel 5300 WiFi cards as transmitters and receivers. VERT2450 dual-frequency antenna by Ettus company, Omnidirectional vertical antenna, 3dBi gain. The CSI tool developed by Halperin was installed on the Lenovo PCs to collect CSI from the receiver. In our experiment, the sampling rate of CSI was set to 1000 Hz to ensure that human activity

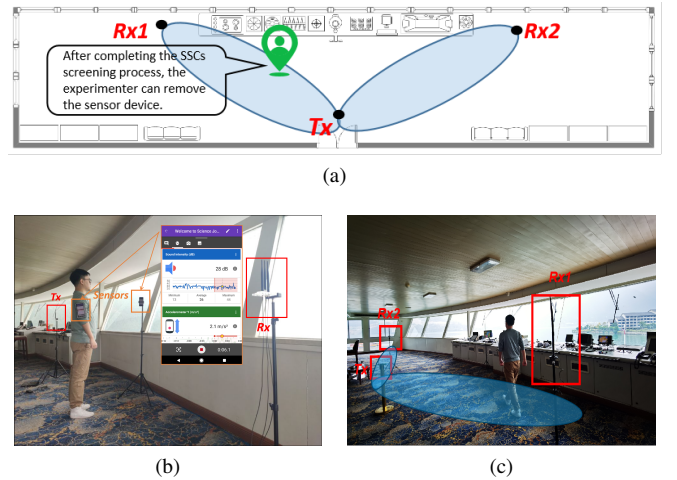


Fig. 12. (a) Test schematic diagram of the experimental scene (Two-link, single person). (b) The sensor equipment was placed on the ship's fixed point and the moving personnel respectively for data acquisition and correlation analysis. (c) Experimental scene of personnel activity detection under Two-link.

could be detected without excessive delay. The sensor data were collected using a smartphone equipped with the Google Science Journal App. We conducted experiments in the ship's main cockpit ($20m \times 6m$) and set up three WiFi link layout methods to verify our proposed framework. Fig. 12 shows the experiment of a single person acting in a Two-link scenario, including the process of SSCs selected.

A. Experimental Results and Performance Analysis of Sensitive Subcarrier Filtering Method

Training phase: First, CSI data were collected when there was no movement in several scenarios, and the collection time was approximately one hour. A total of 6000 data sets of 1 minute in length were isolated for training. Then, we collected CSI data under the influence of human movement, arrange the experimenter to conduct random activities within the antenna range according to the characteristics of the watchkeeper, and finally collected personnel data in three scenes. For the CSI data during movement and during periods without movement, these two types of data were processed by the abovementioned feature value extraction and classification steps to construct a mobile personnel detection classification model. We only collected CSI data when one person was in motion because more people will inevitably have a greater impact on the CSI data. The purpose of this experiment is to verify the effect of distinguishing between the ship's inherent environment and the activities of the human in it after the SSCs selecting process is added to the system through the detection of the manned/unmanned environment in the ship's interior.

Testing phase: This phase collects the test data to test the accuracy of the classification model generated in the training phase. To verify the universality of the model, we chose to collect CSI data in cases ranging from no people to multiple people. A total of up to four people were reached; thus, the final test data set includes the CSI data of 0 to 4 people in three scenarios.

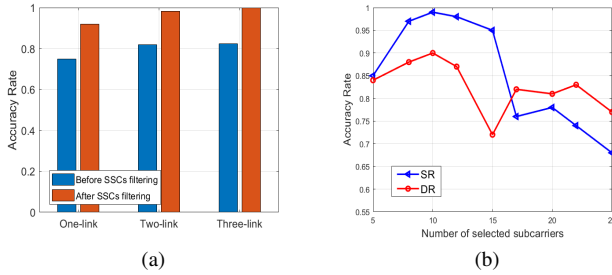


Fig. 13. (a) Influence of sensitive subcarrier selection on detection accuracy. (b) Influence of the selected number of subcarriers on detection accuracy. When the number of selected subcarriers is 10, the accuracy rates of SR and DR are both at a relatively high level.

The accuracy of the personnel movement detection algorithm is defined by the following two quantities: (1) **Static Rate (SR)**, which can accurately detect the probability that there is no human movement in the environment; (2) **Dynamic Rate (DR)**, which can accurately detect the probability of human movement exist in the environment.

The accuracy rate refers to the ratio of the number of samples successfully detected to the total number of samples, and the total number of samples is related to the selection of the time window.

1) Sensitive Subcarrier Filtering on Detection Accuracy:

First, we evaluated the impact of the selection of sensitive subcarriers on the accuracy of human movement detection. Based on the same training and test datasets, we performed a set of experiments that directly used all 30 subcarriers to construct a classification model, and then used 30 subcarriers. The test dataset of the carrier performs the performance test on the classification model, while the other group uses the subcarrier sensitivity evaluation model to select the 10 groups of subcarriers with the highest sensitivity from the training and test datasets to construct and classify the classification model. Finally, in evaluating the effect based on the data from the single-link, dual-link, and triple-link scenarios, the accuracy of human movement detection before and after the selection of sensitive subcarriers is obtained. The results are presented in Fig. 13(a). Before subcarrier selection, the detection accuracies of the three scenes were 75.54%, 80.98%, and 81.24%, respectively, and remained at approximately 80%. After the sensitive subcarriers were selected, the accuracies of each scene increased to 93.06%, 98.21% and 99.84%, the detection accuracy rate improved to more than 90%, and the accuracy rate in the dual-link and triple-link cases is close to 100%. When using the sensitive subcarrier selection, the detection accuracy rate becomes very large. Therefore, it can be concluded that the detection accuracy of human movement can be greatly improved by selecting subcarriers that are more sensitive to human activities.

2) Different Number of Sensitive Subcarriers:

We verified that selecting subcarriers that are more sensitive to personnel activities can improve the accuracy of personnel movement detection, but when an appropriate number of sensitive subcarriers is selected, the accuracy of personnel movement detection is improved the most. This section analyzes this problem. From a theoretical analysis, the fewer subcarriers filtered, the

greater the fluctuation of the information contained in the subcarriers, which is more beneficial for judging the situation when people are moving in the environment. However, when the number of subcarriers filtered is too small, it will destroy the integrity of the original CSI data information, making it impossible to reflect the true environmental characteristics. For example, when there is no human movement, the fluctuation of the selected sensitive subcarriers is mainly caused by environmental factors such as the ship itself, rather than human factors, which ultimately leads to personnel being miscounted by the motion detection algorithm. To verify this theory, we constantly changed the number of sensitive subcarriers to evaluate the accuracy of the human movement detection algorithm. The results are shown in Fig. 13(b). The nine sensitive subcarriers 5, 8, 10, 12, 15, 17, 20, 22, and 25 were selected. We obtained the classification accuracy in each case; it can be seen that starting from 25, as the number of selected sensitive subcarriers is reduced to 12, the accuracy increases from 70% to more than 90%, reaching a peak value, and then when the number of selected subcarriers continues to decrease to 8, the detection accuracy begins to decrease. When the number of selected subcarriers is between 10 and 12, the detection accuracy can be maintained at a high level. Experiments have verified that when the number of selected subcarriers is too large or too small, it has an adverse effect on human movement detection. When the selected number is approximately 10, the detection accuracy can reach the best value.

B. Experimental results and Performance Analysis of Crowd Counting Methods

1) *Overall System Performance Analysis:* We conducted this experiment in the cockpit of a ship to verify the effectiveness of the method for estimating the number of personnel. We have collected a total of 3000 sets of unmanned activities CSI data in ships under different sailing conditions, which are used to observe the dynamic signal characteristics of the ships environment and select SSCs. At the same time, we collected 6000 sets of CSI data when 1 to 4 people were watchkeeping, and 4500 data packets were used as the training data set. Another 1500 packets were used as test datasets, the length of the sliding window was set to 30, and their time-frequency characteristics were extracted according to the above method. In order to ensure the reliability of training samples, when collecting wireless data of multi-person activities, the video data is collected at the same time. After synchronizing the timestamps, we use YOLO [34] technology to automatically label the CSI data sets of different people. Based on the eigenvalues obtained from the training data, a fingerprint database for matching the number of personnel was constructed using the support vector regression algorithm. Then, the regression model was verified using the characteristic values obtained from the test data. The experimental results are presented in Table 1. and Fig. 15. It can be seen that when the number of personnel is small, the recognition accuracy of the number of personnel can reach 90%. As the number of personnel increases, the detection accuracy rate shows a downward trend.

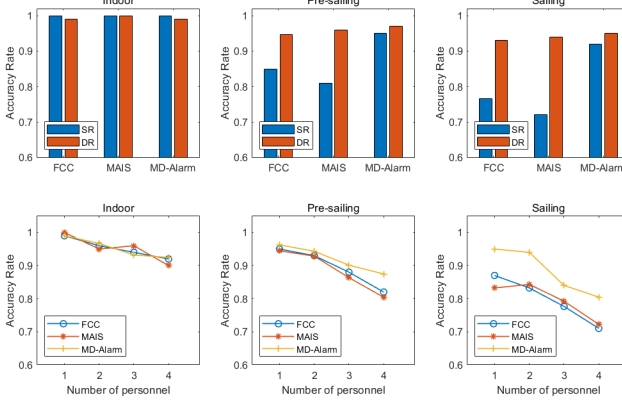


Fig. 14. Comparison of human detection accuracy of three techniques in three different scenarios.

When the number of personnel reaches four, the recognition accuracy rate can still be maintained above 80%. During the actual voyage of a ship, the driving group usually consists of a helmsman and 1-2 watch officers (usually including the master or first officer at a higher management level). Only in certain specific cases, there may be pilots entering the bridge to participate in the command of the berth/enter port the ship. Therefore, the performance of our system is to meet the accuracy requirements of ship bridge watchkeeping detection.

Two methods are compared with MD-Alarm: FCC [20] and MAIS [35]. We tested these methods using three datasets from different scenario states, and the results are presented in Fig.14. First, we describe the true/false-positive rates of the above methods for detecting human activities by SR/DR. It can be seen that when the scene is in the general indoor state, all three methods reflect extremely high accuracy rates, all above 99%. When the scene is switched to the ship interior, the accuracy of all three methods decreases to different degrees due to the sailing state of the ship. Especially due to the influence of ship movement, the false positive rate has increased significantly. Among them, MD-Alarm is more resistant to the dynamic environment, the accuracy of detecting personnel activities is maintained at a high-performance level even under the ship sailing state.

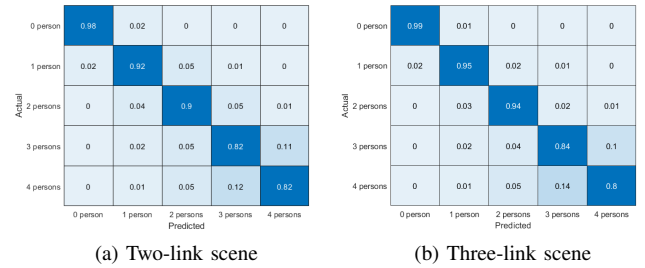
Furthermore, we present the accuracy rate of the three methods for detecting the number of people in different scenarios. In all scenarios, the accuracy of the above three methods will decrease as the number of active personnel increases. When the ship was preparing and starting to move, the accuracy of the FCC and MAIS were significantly reduced. In contrast, because MD-Alarm selects information that is more sensitive to active personnel in a dynamic environment, it still maintains a high crowd counting accuracy rate.

2) Influence of Matrix Expansion Radius R: We have already demonstrated in Section V.B that the expansion radius of the matrix determines the growth rate of the PER, which has a greater impact on the detection accuracy. Therefore, this study tested the change in the PER for different matrix expansion radii, and the results are shown in Fig 16.

We found that there was a significant difference in the PER

TABLE I
ACCURACY RATE OF CROWD COUNTING METHOD

	One-link	Two-link	Three-link
1 person	90%	92%	95%
2 persons	86%	90%	94%
3 persons	72%	82%	84%
4 persons	76%	82%	80%



(a) Two-link scene

(b) Three-link scene

Fig. 15. Confusion matrix.

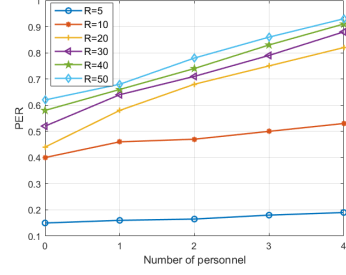


Fig. 16. Effect of expansion radius R on PER.

change under different expansion radii. When the expansion radius was small ($R=5$), the PER was maintained at a small value, and as the number of people increased, the PER change was not obvious. When the radius was moderate ($R=20$), the PER showed a more obvious growth trend with the increase in the number of personnel; when the expansion radius was too large ($R=30$ to 50), the PER increased too quickly and reached personnel more quickly. The upper limit of the quantity estimation also caused a large error in the detection accuracy. Therefore, in general, it is more appropriate to select a matrix expansion radius of about 20.

VII. CONCLUSIONS

In this paper, we provide MD-Alarm, a privacy-protecting and inexpensive ship bridge manpower detection system based on WiFi channel state information. According to the fact that changes in the number of moving people will cause fluctuations in CSI amplitude values and changes in channel delay, a method for estimating the number of people based on channel state information is designed and implemented. This method uses the matrix expansion algorithm to quantify the fluctuation characteristics of the CSI amplitude value to estimate the number of personnel. The results show that the detection accuracy of the number of personnel in various environments can reach more than 80%. This meets the demand for personnel estimation in ship environments. Although the system still has

some deficiencies, such as the requirements of initial training data and equipment layout, there are certain restrictions on the versatility of the system, or the recognition rate of static people is not satisfactory, but this paper is the first attempt to use CSI to detect the number of people in a complex dynamic indoor environment, this provides support and possibility for the application of wireless sensing technology in complex and dynamic indoor environments.

VIII. ACKNOWLEDGMENTS

This work was supported in part by the National Natural Science Foundation of China (NSFC) under Grant No.51979216, in part by the Natural Science Foundation of Hubei Province, China, under Grant 2021CFA001, and in part by Green Intelligent Inland Ship Innovation Programme.

REFERENCES

- [1] M. A. I. Branch, C. House, and C. Place, "Bridge watchkeeping safety study," *Department for Transportation, Marine Accident Investigation Branch, Southampton*, 2004.
- [2] H. Gale and D. Patraiko, "Improving navigational safety," *Seaways*, July, 2007.
- [3] R. Phillips, "Sleep, watchkeeping and accidents: a content analysis of incident at sea reports," *Transportation research part F: traffic psychology and behaviour*, vol. 3, no. 4, pp. 229–240, 2000.
- [4] F. Wang, F. Zhang, C. Wu, B. Wang, and K. J. R. Liu, "Respiration tracking for people counting and recognition," *IEEE Internet of Things Journal*, vol. 7, no. 6, pp. 5233–5245, 2020.
- [5] S. Li, X. Li, K. Niu, H. Wang, Y. Zhang, and D. Zhang, "Ar-alarm: An adaptive and robust intrusion detection system leveraging csi from commodity wi-fi," in *International conference on smart homes and health telematics*. Springer, 2017, pp. 211–223.
- [6] Y. Wang, K. Wu, and L. M. Ni, "Wifall: Device-free fall detection by wireless networks," *IEEE Transactions on Mobile Computing*, vol. 16, no. 2, pp. 581–594, 2016.
- [7] X. Niu, S. Li, Y. Zhang, Z. Liu, D. Wu, R. C. Shah, C. Tanriover, H. Lu, and D. Zhang, "Wimonitor: Continuous long-term human vitality monitoring using commodity wi-fi devices," *Sensors*, vol. 21, no. 3, p. 751, 2021.
- [8] P. Deseck, *International Regulations for Preventing Collisions at Sea*. Barker & Howard, 1983.
- [9] Y. Zheng, Y. Zhang, K. Qian, G. Zhang, Y. Liu, C. Wu, and Z. Yang, "Zero-effort cross-domain gesture recognition with wi-fi," in *Proceedings of the 17th Annual International Conference on Mobile Systems, Applications, and Services*, 2019, pp. 313–325.
- [10] Z. Wang, K. Jiang, Y. Hou, W. Dou, C. Zhang, Z. Huang, and Y. Guo, "A survey on human behavior recognition using channel state information," *Ieee Access*, vol. 7, pp. 155986–156024, 2019.
- [11] Z. Dong, L. Kong, P. Cheng, L. He, Y. Gu, L. Fang, T. Zhu, and C. Liu, "Repc: Reliable and efficient participatory computing for mobile devices," in *2014 Eleventh Annual IEEE International Conference on Sensing, Communication, and Networking (SECON)*. IEEE, 2014, pp. 257–265.
- [12] J. Liu, H. Liu, Y. Chen, Y. Wang, and C. Wang, "Wireless sensing for human activity: A survey," *IEEE Communications Surveys & Tutorials*, vol. 22, no. 3, pp. 1629–1645, 2019.
- [13] M. Chen, K. Liu, J. Ma, Y. Gu, Z. Dong, and C. Liu, "Swim: Speed-aware wifi-based passive indoor localization for mobile ship environment," *IEEE Transactions on Mobile Computing*, 2019.
- [14] Y. Ma, G. Zhou, and S. Wang, "Wifi sensing with channel state information: A survey," *ACM Computing Surveys (CSUR)*, vol. 52, no. 3, pp. 1–36, 2019.
- [15] J. Wang, H. Jiang, J. Xiong, K. Jamieson, X. Chen, D. Fang, and B. Xie, "Lifs: low human-effort, device-free localization with fine-grained subcarrier information," in *Proceedings of the 22nd Annual International Conference on Mobile Computing and Networking*, 2016, pp. 243–256.
- [16] S. Zhang, W. Wang, and T. Jiang, "Wi-fi-inertial indoor pose estimation for microaerial vehicles," *IEEE Transactions on Industrial Electronics*, vol. 68, no. 5, pp. 4331–4340, 2021.
- [17] M. Li, Z. Zhang, K. Huang, and T. Tan, "Estimating the number of people in crowded scenes by mid based foreground segmentation and head-shoulder detection," in *2008 19th international conference on pattern recognition*. IEEE, 2008, pp. 1–4.
- [18] C. Xu, S. Li, G. Liu, Y. Zhang, E. Miluzzo, Y.-F. Chen, J. Li, and B. Firner, "Crowd++ unsupervised speaker count with smartphones," in *Proceedings of the 2013 ACM international joint conference on Pervasive and ubiquitous computing*, 2013, pp. 43–52.
- [19] X. Guo, B. Liu, C. Shi, H. Liu, Y. Chen, and M. C. Chuah, "Wifi-enabled smart human dynamics monitoring," in *Proceedings of the 15th ACM Conference on Embedded Network Sensor Systems*, 2017, pp. 1–13.
- [20] W. Xi, J. Zhao, X.-Y. Li, K. Zhao, S. Tang, X. Liu, and Z. Jiang, "Electronic frog eye: Counting crowd using wifi," in *IEEE INFOCOM 2014 - IEEE Conference on Computer Communications*, 2014, pp. 361–369.
- [21] S. Depatla and Y. Mostofi, "Crowd counting through walls using wifi," in *2018 IEEE international conference on pervasive computing and communications (PerCom)*. IEEE, 2018, pp. 1–10.
- [22] S. Di Domenico, G. Pecoraro, E. Cianca, and M. De Sanctis, "Trained-once device-free crowd counting and occupancy estimation using wifi: A doppler spectrum based approach," in *2016 IEEE 12th International Conference on Wireless and Mobile Computing, Networking and Communications (WiMob)*. IEEE, 2016, pp. 1–8.
- [23] M. Chen, K. Liu, J. Ma, X. Zeng, Z. Dong, G. Tong, and C. Liu, "Moloc: Unsupervised fingerprint roaming for device-free indoor localization in a mobile ship environment," *IEEE Internet of Things Journal*, vol. 7, no. 12, pp. 11 851–11 862, 2020.
- [24] U. Singh, J.-F. Determe, F. Horlin, and P. De Doncker, "Crowd forecasting based on wifi sensors and lstm neural networks," *IEEE transactions on instrumentation and measurement*, vol. 69, no. 9, pp. 6121–6131, 2020.
- [25] K. Chen, C. C. Loy, S. Gong, and T. Xiang, "Feature mining for localised crowd counting," in *Bmvc*, vol. 1, no. 2, 2012, p. 3.
- [26] D. Porcino and W. Hirt, "Ultra-wideband radio technology: potential and challenges ahead," *IEEE communications magazine*, vol. 41, no. 7, pp. 66–74, 2003.
- [27] R. M. Haralick, S. R. Sternberg, and X. Zhuang, "Image analysis using mathematical morphology," *IEEE transactions on pattern analysis and machine intelligence*, no. 4, pp. 532–550, 1987.
- [28] P. Nosov, I. Palamarchuk, M. Safonov, and V. Novikov, "Modeling the manifestations of the human factor of the maritime crew," . . . , no. 5 (77), 2018.
- [29] D. Halperin, W. Hu, A. Sheth, and D. Wetherall, "Tool release: Gathering 802.11 n traces with channel state information," *ACM SIGCOMM Computer Communication Review*, vol. 41, no. 1, pp. 53–53, 2011.
- [30] X. Li, S. Li, D. Zhang, J. Xiong, Y. Wang, and H. Mei, "Dynamic-music: accurate device-free indoor localization," in *Proceedings of the 2016 ACM International Joint Conference on Pervasive and Ubiquitous Computing*, 2016, pp. 196–207.
- [31] Y. Xie, J. Xiong, M. Li, and K. Jamieson, "md-track: Leveraging multidimensionality for passive indoor wi-fi tracking," in *The 25th Annual International Conference on Mobile Computing and Networking*, 2019, pp. 1–16.
- [32] M. Kotaru, K. Joshi, D. Bharadia, and S. Katti, "Spotfi: Decimeter level localization using wifi," in *Proceedings of the 2015 ACM Conference on Special Interest Group on Data Communication*, 2015, pp. 269–282.
- [33] Y. Xie, Z. Li, and M. Li, "Precise power delay profiling with commodity wi-fi," *IEEE Transactions on Mobile Computing*, vol. 18, no. 6, pp. 1342–1355, 2018.
- [34] J. Redmon, S. Divvala, R. Girshick, and A. Farhadi, "You only look once: Unified, real-time object detection," in *Proceedings of the IEEE conference on computer vision and pattern recognition*, 2016, pp. 779–788.
- [35] C. Feng, S. Arshad, and Y. Liu, "Mais: Multiple activity identification system using channel state information of wifi signals," in *International Conference on Wireless Algorithms, Systems, and Applications*. Springer, 2017, pp. 419–432.



Mengda Chen received the B.S. degree in electronic information engineering from the Hubei University, China, in 2013, and the M.S. degree in automatic control engineering from the Guilin University of Technology, China, in 2016. He is currently a Ph.D. student in Wuhan University of Technology. His research interests focused on wireless perception and indoor navigation.



Kehao Wang received the B.S degree in electrical engineering, M.S. degree in communication and information system from Wuhan University of Technology, Wuhan, China, in 2003 and 2006, respectively, and Ph.D in the Department of computer science, the University of Paris-Sud XI, Orsay, France, in 2012. From Feb. 2013 to Aug. 2013, he was a postdoc with the HongKong Polytechnic University. In 2013, he joined the School of Information Engineering at the Wuhan University of Technology, where he is currently an associate professor. From Dec. 2015, he has been a visiting scholar in the Laboratory for Information and Decision Systems, Massachusetts Institute of Technology, Cambridge, MA, USA. His research interests are stochastic optimization, operation research, scheduling, wireless network communications, and embedded operating system.



Jie Ma received the Ph.D. degree in computer science from the Huazhong University of Science and Technology, China, in 2010. He is currently an associate professor in the School of Navigation at the Wuhan University of Technology. His research includes networked sensing systems and data driven intelligent transportation systems, supported by National Natural Science Foundation of China. He has published over 20 journal and conference papers in the related fields.



Xuming Zeng received the Ph.D. degree in earth exploration and information technology from the China University of Geosciences, Wuhan, China, in 2018. He is currently a post doctoral fellow in traffic and transportation engineering with the School of Navigation, Wuhan University of Technology, Wuhan. He has been studying wireless ad-hoc network for shipboard environment with the Wuhan University of Technology since 2019. His research interests include routing protocols, MAC, QoS, clustering, and reliable wireless transmission.



Kezhong Liu received the B.S. and M.S. degrees in marine navigation from the Wuhan University of Technology(WUT), Wuhan, China, in 1998 and 2001, respectively. He received the Ph.D. degree in communication and information engineering from the Huazhong University of Science and Techonogy, Wuhan, China, in 2006. He is currently a professor with School of Navigation, WUT. His active research interest include indoor localization technology and data mining for ship navigation.



Mozi Chen received the B.S. degree in electric engineering from the Hubei University of Technology, China, in 2013. He received the M.S. and Ph.D.degree in navigation engineering from the Wuhan University of Technology (WUT), China, in 2016 and 2020. He is currently an associate researcher in WUT. His research work has been focusing on wireless sensing techniques and machine learning algorithms for human localization, emergency navigation and activity recognition in mobile environment, i.e., cruise ships.



Kai Zheng received the Ph.D. degree with the School of Geodesy and Geomatics, Wuhan University, in 2020. He is currently an associate researcher with the Wuhan University of Technology. His research interests are GNSS precise positioning techniques.